



Article

A Detailed Forecast of the Technologies Based on Lifecycle Analysis of GMAW and CMT Welding Processes

André Souza Oliveira ^{1,2} , Raphael Oliveira dos Santos ², Bruno Caetano dos Santos Silva ^{1,2}, Lilian Lefol Nani Guarieiro ^{1,2} , Matthias Angerhausen ³, Uwe Reisgen ⁴, Renelson Ribeiro Sampaio ², Bruna Aparecida Souza Machado ², Enrique López Droguett ⁵, Paulo Henrique Ferreira da Silva ⁶ and Rodrigo Santiago Coelho ^{1,2,*}

- ¹ SENAI CIMATEC, Instituto SENAI de Inovação em Conformação e União de Materiais, Av. Orlando Gomes, 1845, Piatã, Salvador, BA 41650-010, Brazil; andre.soliveira@fieb.org.br (A.S.O.); bruno.silva@fieb.org.br (B.C.d.S.S.); lilian.guarieiro@fieb.org.br (L.L.N.G.)
- ² SENAI CIMATEC, Programa de Pós-Graduação MPDS/GETEC/MCTI—Centro Universitário SENAI CIMATEC, Av. Orlando Gomes, 1845, Piatã, Salvador, BA 41650-010, Brazil; raphaelosantos@gmail.com (R.O.d.S.); renelson@fieb.org.br (R.R.S.); brunam@fieb.org.br (B.A.S.M.)
- ³ Forschungs- und Entwicklungsgesellschaft Fügetechnik GmbH, Driescher Gässchen 5, 52062 Aachen, NRW, Germany; angerhausen@isf.rwth-aachen.de
- ⁴ Institut für Schweißtechnik und Fügetechnik, RWTH Aachen University, Pontstraße 49, 52062 Aachen, NRW, Germany; reisgen@isf.rwth-aachen.de
- ⁵ Departamento de Ingeniería Mecánica, Universidad de Chile, Exibir Comentario, Santiago 837-0456, Chile; enlopez@uchile.cl
- ⁶ UFBA, Departamento de Estatística, Av. Adhemar de Barros, Ondina, Salvador, BA 40170-110, Brazil; phfs205@hotmail.com
- * Correspondence: rodrigo.coelho@fieb.org.br



Citation: Oliveira, A.S.; Santos, R.O.d.; Silva, B.C.d.S.; Guarieiro, L.L.N.; Angerhausen, M.; Reisgen, U.; Sampaio, R.R.; Machado, B.A.S.; Droguett, E.L.; Silva, P.H.F.d.; et al. A Detailed Forecast of the Technologies Based on Lifecycle Analysis of GMAW and CMT Welding Processes. *Sustainability* **2021**, *13*, 3766. <https://doi.org/10.3390/su13073766>

Academic Editor: Bhavik Bakshi

Received: 4 February 2021

Accepted: 23 March 2021

Published: 29 March 2021

Publisher's Note: MDPI stays neutral with regard to jurisdictional claims in published maps and institutional affiliations.

Abstract: In this study, GMAW and CMT welding technologies were evaluated in terms of their technological lifecycles based on their patent datasets together with the S-curve concept, and the joints were evaluated in terms of their welding characteristics. To predict the future trends for both technologies, different models based on the time-series and growth-curve methods were tested. From a process point of view, the results showed better performance and stability for the CMT process based on the heat input to the base material and the frequency of the short circuits. The temperature distribution in the sample revealed that the GMAW process delivers higher values and, consequently, greater heat transfer. Regarding the technological lifecycle, the analyses revealed that the CMT welding process, despite being recent, is already in its mature phase. Moreover, the GMAW welding process is positioned in the growth phase on the S-curve, indicating a possibility of advancement. The main findings indicated that through mathematical modelling, it is possible to predict, in a precise way, the inflection points and the maturity phases of each technology and chart their trends with expert opinions. The new perspectives for analysing maturity levels and welding characteristics presented herein will be essential for a broaden decision-making market process.

Keywords: S-curve; technology lifecycle; GMAW; CMT



Copyright: © 2021 by the authors. Licensee MDPI, Basel, Switzerland. This article is an open access article distributed under the terms and conditions of the Creative Commons Attribution (CC BY) license (<https://creativecommons.org/licenses/by/4.0/>).

1. Introduction

Many developments in joining techniques have emerged to supply the demand for productivity alongside reliability. As one of the most commonly used processes in industry, welding is present in almost all products from the machinery, automotive, shipbuilding, and aerospace fields. Because of the many variables involved (energy sources, modes of operation, productivity, welding position, quality and properties, market strategies, digitalisation, materials development, reliability, costs, etc.) and the existence of many welding processes, choosing a proper welding process has become quite difficult.

Developed in the late 1950s, Gas Metal Arc Welding (GMAW) is one of the most commonly used welding processes in the world due to its high productivity and possibility

of automation, as described in the work of Yapp and Blackman [1]. Some advantages of GMAW are the high deposition rate, low-cost equipment, good welding penetration, use for almost all metals and alloys, use in coating layer application, and good mechanical properties. On the other hand, Shen et al. [2] reported that this process can present unstable arc behaviour, which can impact the reliability and scale up production in some applications. Additionally, the process is sensitive to contaminants, can produce lack of fusion, is less portable when compared to others and is less suited to smaller and constricted spaces due to the nature of the welding touch.

Guided by the challenges of lightweight construction in the automotive and aerospace industries, the demand for development is focused on increasing the materials' strength and improving the joining processes. According to Goede et al. [3], steel remains the primary constituent of vehicles structures. One significant challenge in welding parts is the production of tailored blanks of dissimilar materials, not only between different classes of steels, but also between aluminium and steel. In this regard, Madhavan et al. [4] stated that a low heat input fusion welding process could provide a solution. Low heat input leads to insufficient time for enough materials to melt, and the results are a low volume weld pool with fast freezing. This impacts the dendritic structure and controls the intermetallic layer formation.

Considered a variation of the GMAW process, Cold Metal Transfer (CMT) consists of a power source and a torch with a wire feed speed disassociated from the welding energy, as described in the work of Cornacchia et al. [5]. Despite its electrical current control, this process allows wire retraction during the short circuit transfer. This eliminates the need for an electromagnetic force to detach the molten material of the electrode, which results in a low-spatter or spatter-free procedure. According to Selvi et al. [6], with a transfer mode under a low voltage, the heat input on the welded part is also decreased.

There are notable studies on the arc characteristics of the CMT process. For instance, Zhang et al. [7] investigated the arc and metal transfer behaviours in the CMT welding of aluminium and zinc-coated steel. The results showed that a low heat input and spatter-free welding, characteristics of CMT processes, can improve the mechanical performance of dissimilar material joining. Focusing on this issue, Pickin et al. [8] used the advantages of the CMT process for low dilution cladding applications and showed that the process's characteristics and control can optimise crack formation during solidification due to eutectic reactions. In another study, Costa et al. [9] analysed the arc characteristics and best practical parameters involving standard GMAW and its derivative processes with the short-circuit transfer mode, including the CMT. It was shown that the lower heat input delivered in the CMT configuration can be more efficient in some welding positions, improving the root characteristics of the joint.

Although many studies have been presented, there is still a lack of information and research materials for the CMT process compared to standard ones, such as GMAW, especially when not only basic characteristics (level of heat input and its impact on the delivered temperature and material deposition) but also technological trends are addressed. Chang et al. [10] noted that the evaluation of welding technologies from a technical perspective has fundamental importance in establishing the limits of the process parameters. However, besides the technical aspects of the parameters and setup, it is also important to incorporate a broader perspective to facilitate a multidisciplinary view of this analysis, such as the Technology Lifecycle (TLC) approach.

2. The TLC Approach Based on the S-Curve Concept

TLC analyses have been applied for different purposes and are delineated into several phases, such as embryonic, growth, maturity, and aging, as stated by Taylor and Taylor [11]. Wilder et al. [12] showed that S-curve models can facilitate the understanding of change dynamics, reveal patterns and technological changes, and serve as tools combined with growth models to predict inflection points and thus establish monitoring strategies. The model proposed in this study originates from the established S-curve concept proposed

by Little [13] to measure technological changes and provide an analytical method for the adaptation of strategic planning techniques to manage corporate R&D resources. In addition to the TLC study, it is essential to note that the use of patents is an important strategy to study and explore the forces that drive sustainable development, as the study of Wu et al. [14] addressed.

Figure 1, provided by Gao et al. [15], represents the S-curve within the category of nonlinear growth curve models, which has been extensively applied in other scientific disciplines, such as biology and medicine. For instance, Xinán and Aijun [16] identified the non-linear growth model that provides the best fit for determining the growth rate and established mathematical formulae to explore the growth intervals of a rapidly growing turbot fish strain. The technological trends were categorized into four different stages (emerging, growth, maturity, and saturation), which represent, respectively, low and high competitive impact, the key technology, and, finally, the phase at which the technology begins to be replaced, as noted by Madvar et al. [17].

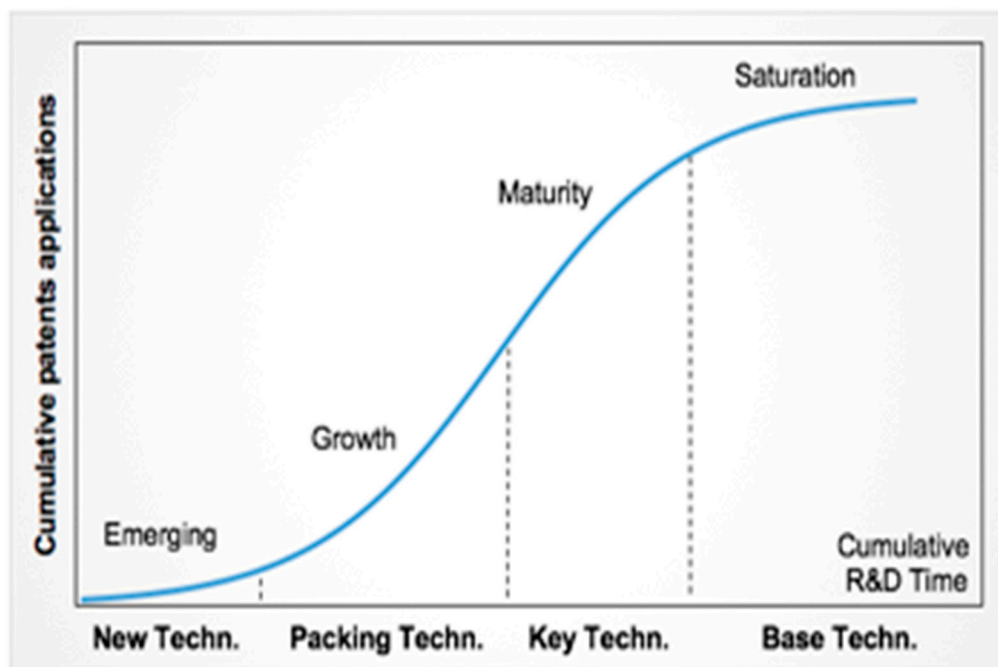


Figure 1. The S-curve concept of the Technology Lifecycle (TLC). Adapted from [15].

According to Gao et al. [15], the dominant approach for analyzing TLC uses the S-curve to observe patent applications over time, and this kind of analysis helps decision-makers estimate future development trends and, thus, mitigate risks and increase the probability of success. Studies based on the S-curve can use different approaches, such as conceptual and visual approaches, as demonstrated by the study of photovoltaic technology competitive strategies proposed by Jamali et al. [18]; however, this methodology carries significant uncertainty. The use of mathematical (or statistical) modelling has increased and seems to be more promising for predictions when an event will occur and can be combined with expert opinions to predict if an event will occur, as noted by Fye et al. [19]. For this type of modelling, the historical data of patents and scientific studies (articles, reports, and publications) have become reliable references to estimate future development [20].

Nevertheless, there is still room for improvement, such as identifying all points of transition between stages. In this regard, Andrade et al. [21] sought to identify these transition points using an empirical approach, but this approach seems to be inaccurate. In the same sense, Yang et al. [22] used the concept of the S-curve for an important analysis of the competitiveness of several countries in the graphene industry. However, it presents only a visual analysis of the S-curve so that it can lead to inadequate interpretation.

Wilder et al. [12] used mathematical modelling to define the central inflection, but the S-curve has three inflection points. On the other hand, Kucharavy and De Guio [23] made some advances but were still limited to a specific model, such as the logistic growth-curve.

De Gooijer and Hyndman [24] revealed that the use of more advanced smoothing and forecasting techniques presented in other studies may offer more robust solutions, such as using a time-series divided into exponentials, ARIMA, and automatic ARIMA (or Auto-ARIMA). Xin'an and Aijun [16] suggested another option: the use of growth-curves with different models, such as exponential, Gompertz, Chapman–Richards, and logistic models.

Past time-series methods were very subjective, but, with the introduction of more advanced models like ARIMA, they now provide the necessary mathematical rigour, allowing them to represent patent evolution, as established by Smith and Agrawal [20]. Krispin [25] considers time-series techniques to be essential for statistical programming, and Fye et al. [19] noted that time-series methods can be used extensively, although they may lose accuracy over a long-time horizon. Bouzada [26] noted that, in general, the classical time-series decomposition method considers the following characteristics: seasonality, trends, cycles, and random components. Kabacoff [27] stated that these methods can produce good short-term forecasts in a wide range of applications despite their simplicity. On the other hand, growth-curve methods have also been used to predict bacterial growth, as studied by Lobacz et al. [28], in a microbiology model to describe this phenomenon accurately in cheese production. In relation to technological forecasting, these models have been applied to patent datasets to determine the maturity of new technologies, such as additive manufacturing [29].

This work proposes to analyse the basic aspects of the joints produced by the CMT and GMAW welding processes and mainly to exploit the technological trends based on patents and expert opinions to predict a forecast for each technology. Firstly, the main goal is to correlate the heat input and welding characteristics using the same wire and setup to join non-alloy quality structural steel (ISO E235B) in terms of its temperature reached and welding penetration. The main focus of the following TLC analyses is to investigate different techniques applied to specific boundary conditions to provide a representative analysis of the chosen welding technologies' maturity levels.

3. Materials and Methods

3.1. The Welding Analyses

3.1.1. Sample Preparation

The welds investigated in this work were prepared in the V-joint configuration without any root openings and a groove angle of 60°. The processes of GMAW and CMT were used to join 5-mm-thick ISO E235B [30] steel with dimensions of about 100 mm in width and 250 mm in length. The chosen process parameters were monitored using a YOKOGAWA DL850 data acquisition recorder (YOKOGAWA, Tokyo, Japan). The joints were prepared using a standard filler, G3Si1 (ER70S-6), with a 1.2 mm diameter in three passes, and no backing bar was used. Samples of 200 × 250 × 5 mm³ were prepared for each process, described as GMAW and CMT. Tables 1 and 2 show the chemical composition and the mechanical properties, respectively, of all materials used in this work.

Table 1. Chemical composition (wt%) of the materials used in this work, according to manufacturer.

	C %	Mn %	Si %	S %	P %	Cu %
ISO E235B	0.17	1.40	0.40	0.045	0.045	-
G3Si1 (ER70S-6)	0.07	1.40	0.80	0.012	0.012	0.10

Table 2. Mechanical properties of the materials used in this work, according to manufacturer.

	Rp0.2 (MPa)	Rm (MPa)	A (%)
ISO E235B	235	340–470	26
G3Si1 (ER70S-6)	470	560	26

As a power source, we used a Fronius TransPuls Synergic 4000 CMT R machine. The samples were manufactured with the synergic mode turned on, which means that only the parameter Wire Feed Rate (WFR) was set in the power source control. This allowed for better control of the parameters and ensured a uniform penetration and weld bead profile. For comparison purposes, the joints were prepared using the same voltage and welding travel speed. The values of the current were different to explore the differences in the wire feed. Thus, the heat input of the CMT process was slightly higher. Table 3 shows the applied welding parameters and the estimation of the heat input considering a welding process efficiency of about 85% for both the GMAW and CMT processes in accordance with the studies carried out by Haelsing et al. [31] and Pepe et al. [32]. The heat input was calculated according to Equation (1):

$$Q = \frac{60 \times U \times I}{1000 \times v} \quad (1)$$

where Q is the heat input (kJ/mm), U is the voltage (volts), I is the current (ampere), and v is the travel speed (mm/min).

Table 3. Setup welding parameters.

Sample	Voltage (V)	Current (A)	Wire Feed (m/min)	Travel Speed (mm/min)	Heat Input (kJ/mm)
GMAW	18.5	198	5.0	400	0.55
CMT		229	8.0		0.65

All samples were manufactured and characterised at the Institute for Welding and Joining at the University of Aachen (RWTH Aachen, ISF) in Germany.

3.1.2. Temperature Measurements

To determine the temperature distribution during the process, standard thermocouples of type-k were installed on the bottom sides, in the middle of the joint length, at three different points from the centreline: 2, 4, and 6 mm. The data recording and analyses were performed using the DIAdem[®] software, and the Short Circuit Frequency (SCF) was determined by applying a Fast Fourier Transform (FFT) based on all three welding pass curves for both current and voltage (arithmetic average). The SCF analysis was used to verify if the material deposition occurred in a standard way and if it corresponded to a certain regular frequency.

3.1.3. Welding Characterisation

The weld penetration and shapes were measured using the ImageJ[®] software based on optical macrographs taken from the transversal cross sections. The samples were ground, polished, and etched using Nital 5%. The area was estimated using the average of all three passes. The real wire feed (m/min) of each process was then calculated based on the real microstructural dimensions in accordance with Equation (2):

$$WFR = \frac{A \times v \times 4}{\pi \times d^2} \quad (2)$$

where WFR is the wire feed rate (m/min), A is the average cross sectional area of the deposited material (mm^2), v is the welding (travel) speed (mm/min), and d is the wire diameter (mm), as proposed by Imoudu et al. [33]. Additionally, the dilution was calculated based on the estimated areas measured in the macrographs, according to Tomków et al. [34], dividing the molten area of the base material by the total molten area of the joint.

3.2. TLC Analyses of Technological Maturity

To understand the maturity and stage of development for each welding technology, different statistical models were used to assess and predict future trends. Here, the analyses and assessments followed consolidated references from statistical studies and consisted of (i) data collection and preparation, (ii) statistical model development and tests, and (iii) analyses and comparisons of the results, as suggested by Kabacoff [27].

3.2.1. Data Collection and Preparation

All data used in this work were collected using the patent research and analytics platform Derwent Innovation™, a Clarivate Analytics company. In particular, the Global Patent Data Collection was accessed on July 14th 2020 (8:49 pm Brazilian time) using the Text-Fields option in the Derwent Innovation Index (DII) database. The analyses were conducted at SENAI CIMATEC—Salvador, Bahia, Brazil, which holds the license for use. The first challenge was to select keywords that represent the different ways in which the technologies of interest could be found in the documents. The DII database stores patents that have been deposited worldwide. The survey was carried out by searching for the terms selected in the title, abstract, and claims of the patent documents. The following queries were the references needed to obtain each database related to the GMAW and CMT patent documents and were entered in the “Preview/edit queries” field:

- GMAW technology: $AB = ((\text{gmaw OR (gas ADJ metal ADJ arc ADJ welding)}) \text{ AND welding}) \text{ OR } AB = ((\text{mag OR (metal ADJ active ADJ gas)}) \text{ AND welding}) \text{ OR } AB = ((\text{mig OR (metal ADJ inert ADJ gas)}) \text{ AND welding}) \text{ NOT } AB = ((\text{cold ADJ metal ADJ transfer})) \text{ NOT } AB = (\text{cmt});$
- CMT technology: $AB = ((\text{cold ADJ metal ADJ transfer})) \text{ OR } AB = ((\text{cmt})) \text{ AND } AB = (\text{welding}) \text{ NOT } AB = ((\text{mag OR (metal ADJ active ADJ gas)})) \text{ NOT } AB = ((\text{mig OR (metal ADJ inert ADJ gas)}))$.

Notably, these patent databases can have an 18-month restriction in their access period that precedes the full publication of a patent in most countries [35]. The preparation of the dataset started with the use of patents accumulated each year according to each selected technology and following the S-curve model (assessed by the priority date). The dataset was then organised with the number of patents for each year, with a value of zero used for patents without any deposit date of reference.

3.2.2. Statistical Model Development and Tests

The statistical models applied in this work were developed and analysed in the R Studio environment [36], which was used to import the dataset, generate the plots, and analyse the results. Time-series and growth-curve models were applied to analyse the patent evolution and exploit the technological trends:

- Time-series: The forecast (8.11) package developed by Hyndman et al. [37], which contains methods for smoothing and forecasting using time-series analysis and linear models;
- Growth-curves: The growthrates (0.8.1) package developed by Petzoldt [38], which includes nonlinear growth models with varying quantities of parameters written as analytical solutions of the differential equation.

Different mathematical and statistical algorithms were evaluated for each model. Table 4 summarises each model’s characteristics (both time-series and growth-curve models) used in this study. In general, for the algorithms used in the growth-curve models,

it is necessary to engage in some initial interactions to establish the starting values for each model's parameters. By doing so, it is possible to better optimise the results. In general, models with up to three parameters work well with single starting values. On the other hand, for models with more than three parameters, such as Gompertz, Richards, and Baranyi, it is necessary to establish data ranges with minimums and maximums for each parameter to avoid alerts.

Table 4. Summary of all models used in this study to obtain the best fit for each patent's data.

	Model	Description
Time-series	Exponential Single	Exponential smoothing methods were originally used in the 1950s as a collection of ad hoc techniques for extrapolating various types of univariate time series [20]. The Holt–Winters exponential single model is indicated for univariate data without a trend or seasonality [39].
	Exponential Double	Holt–Winters exponential smoothing that adds support for trends in the univariate time-series [39].
	Exponential Triple	Holt–Winters exponential smoothing that adds support for seasonality in the univariate time-series [20], which likely does not fit well since the S-curve has no seasonality.
	ARIMA and Auto-ARIMA	The autoregressive integrated moving average for forecasting discrete time-series processes, and Auto-ARIMA fits the best ARIMA model to the univariate time series easily [39].
Growth-curve	Logistic	The simplest mathematical function that produces an S-curve with three parameters for studying and forecasting future changes. The application of the logistic curve can contribute essentially to the accuracy of a long-term forecast [40].
	Gompertz	Originally derived to estimate human mortality with three parameters, and there are a number of different ways that this equation can be written with three or four parameters [41].
	Richards	The generalisation of a logistic curve that is no longer symmetrical around the point of inflection, with four parameters [41].
	Baranyi	Developed for predicting the bacterial growth curve; this is a dynamic model with four parameters dealing with time-varying environmental conditions [42].
	Exponential	Classical growth model with two parameters and a very simple structure [43].

Models using time-series are more easily adjusted because the algorithm seeks to adjust the data characteristics to each time-series model. In general, errors can occur if it is not possible to adjust the curve—for example, trying to adjust data that does not have seasonality in a model that requires seasonality. In this way, the algorithm produces alerts that cannot be adjusted. After attending to these observations and interactions and considering the exceptions of the time-series models mentioned above, the algorithms no longer generated alerts.

The next step was to plot each graph to compare the actual curve with the predicted one. This procedure was necessary because, although the algorithm did not emit more alerts, the resulting curves may not have fit into the original curves. If there were still some distortions in this visual inspection, it would be necessary to change the model's initial parameters again and rerun the algorithm.

3.2.3. Analyses and Comparisons between the Models

Best model analysis began by selecting the best smoothing method for evaluating the level of statistical representativeness, evaluating the accuracy measurement, and determining the information quality based on the principle of parsimony, as discussed in Bozdogan [44]. Afterwards, a prediction test was carried out with the existing data, removing the last three years from the dataset. Then, new smoothing of the data prediction was generated to compare the predicted and observed datasets.

Based on the best prediction model, a full dataset was used to forecast the technological development for the following years. Notably, for the growth-curve model, it was necessary to identify the curve parameters. The summary(.) command was included in the

algorithm developed in the *growthrates* package to identify these parameters. Then, the corresponding equation was defined and, by obtaining the 2nd and 3rd order derivatives, established the inflection points, as detailed in Section 3.2. Finally, when discussing trends and using expert opinions on welding technologies, it is crucial to check the results and identify factors likely to alter the development suggested by the TLC [15].

4. Results and Discussion

4.1. Welding Analyses

The chosen process parameters ensured a good welding bead with a lack of superficial defects and discontinuities under both processes. Visual analyses highlighted the characteristics of CMT welds to have a slightly more pronounced bead compared to standard GMAW, which is expected due to the low heat input, fast solidification, and higher deposition ratio, as also observed in the research carried out by Selvi et al. [6]. The characteristic curves for current and voltage were monitored and are presented in Figure 2 for both processes. Based on the curves for standard GMAW shown in Figure 2a,b, standard behaviour with peaks of current occurs when the arc reignites after the short circuit phase. At this point in time, the droplet touches the base metal, and the material detaches from the wire tip (nip-off) due to the magnetic forces, as also reported by Selvi et al. [6]. For the CMT welds, the current curve showed the three phases (I, II, and III) characteristic of this process, in accordance with the results obtained by Zhang et al. [7] and Mezrag et al. [45] (Figure 2c). It can be observed that on the high peaks of the current (phase I in Figure 2c), the arc reignites, and the filler material melts. This peak time is followed by the background time (phase II in Figure 2c), when a small droplet of molten metal grows on the tip of the wire and is followed by a voltage reduction at this moment, which is also in accordance with the results of Zhang et al. [7]. This process occurs under small current values to inhibit the globular transfer of material. At the end of the cycle, short circuit transfer (phase III in Figure 2c) occurs, and the voltage decreases. Notably, molten material detachment does not occur due to magnetic forces but because of wire feed retraction. Similar results were reported by Zhang et al. [46], who investigated the effects of welding velocity on the microstructural formation of AZ31 Mg alloy material cladding using the CMT process. The authors observed that after the arc ignition, a period of a peak pulse occurred, causing the wire electrode to melt. Then, there was a period of a pulse base with a lower welding current and a decrease in the arc intensity.

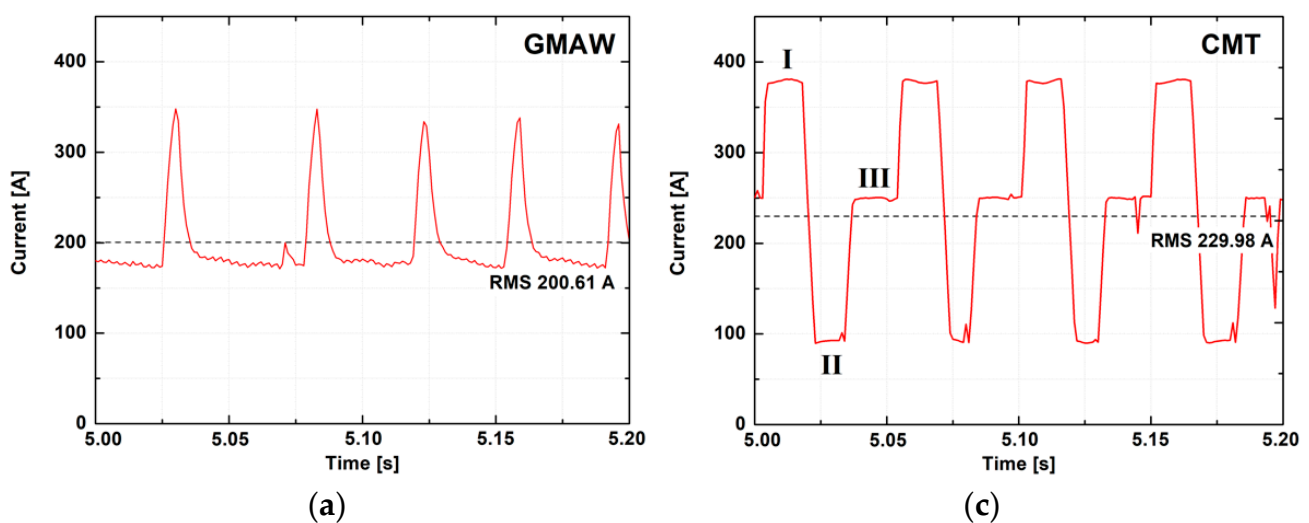


Figure 2. Cont.

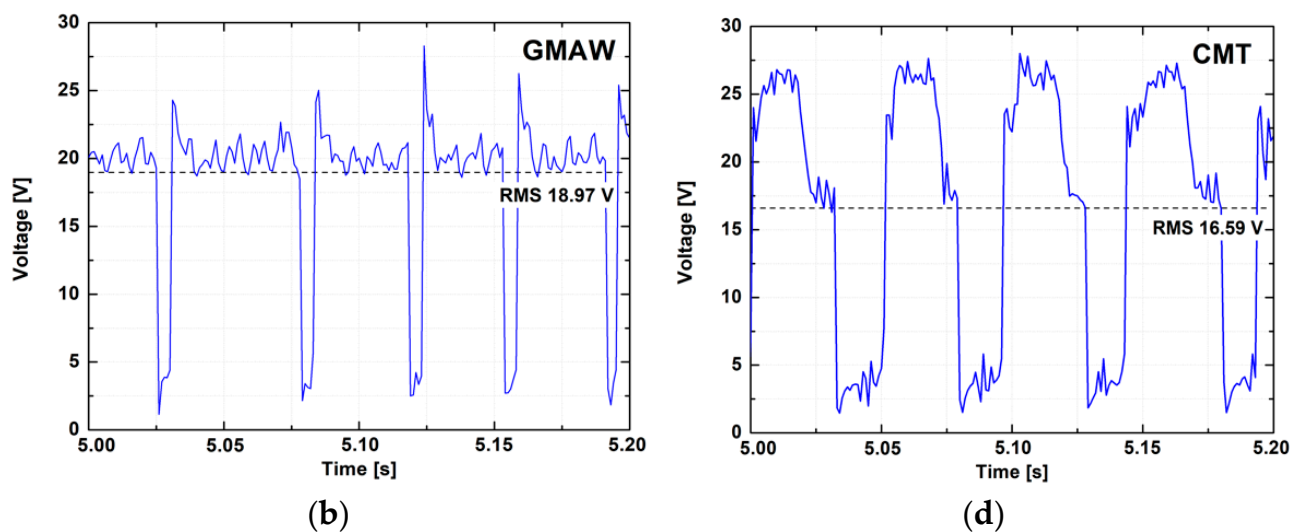


Figure 2. Characteristic curves of the current and voltage for standard Gas Metal Arc Welding (GMAW) (a,b); and for the Cold Metal Transfer (CMT) process (c,d).

Comparing the characteristic curves of both processes, CMT presented a smaller average (Root Mean Square, RMS) welding voltage during the procedure, which means that the arc of this technology is also smaller than that of standard GMAW, which has a positive impact on the heat input yield. These characteristics are in accordance with the results obtained by Dutra et al. [47]. It was reported that the short-circuit voltage remains at a very low level during this process when compared to GMAW-MIG technology. As a result, the energy decreases and remains constant. Additionally, the CMT process reaches higher current values for short periods of time, while the peaks for standard GMAW process are shorter and instantaneous—just enough to reopen the arc. In this case, the current oscillation can be attributed to the power source response control, behaviour that can also be observed in each phase (I, II, and III) of the CMT process. In accordance with Selvi et al. [6], a higher peak of current in the CMT process can also contribute to a higher deposition rate, as shown in Table 5.

Table 5. Measured welding parameters for both processes, standard GMAW and CMT.

Sample	Voltage (V)	Current (A)	Wire Feed * (m/min)	Travel Speed (mm/min)	Heat Input (kJ/mm)
GMAW	18.97	200.61	6.39	400	0.57
CMT	16.59	229.98	8.17	400	0.57

* Based on metallographic analyses presented later in this section (Figure 5, Table 7, and Equation (2)).

Another significant characteristic of the CMT process is its stability and pronounced SCF. Figure 3 shows the FFT graphs for both processes side-by-side, and Table 6 highlights the almost constant values of SCF for the CMT process in each pass. The average value is also presented and confirms the stability of the process. The distinguish peaks of the SCF control, through digital process, the power supply and the retraction of the wire, thereby ensuring the stability and deposition control of the CMT process. Note that this is not clear for the standard GMAW process, where no dwell-defined peaks of frequency were detected.

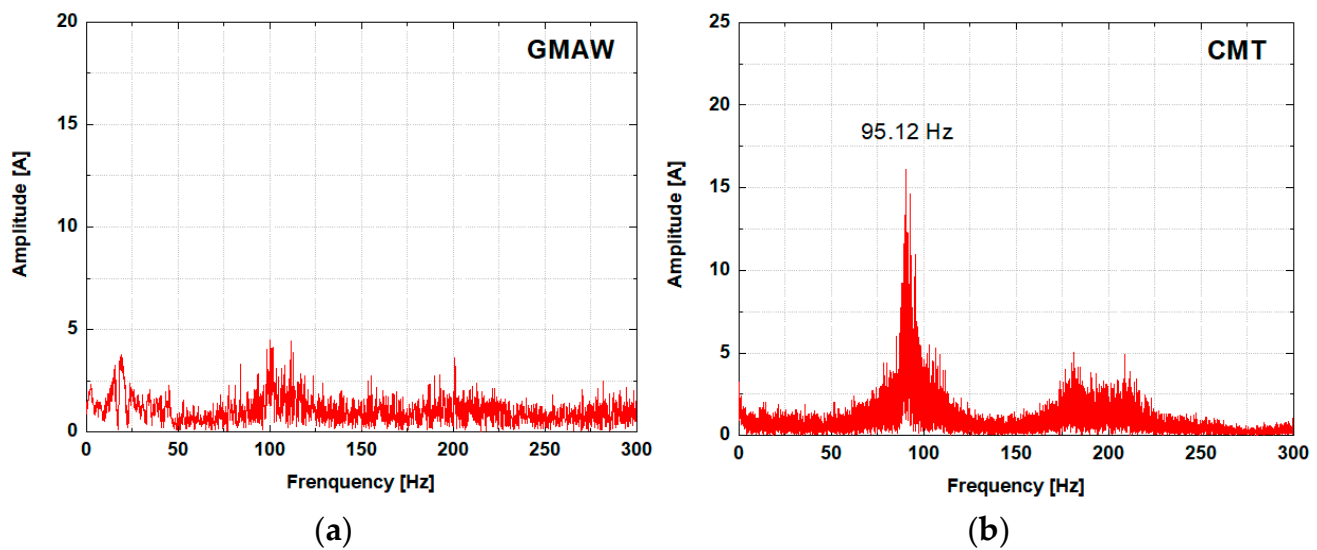


Figure 3. Typical FFT graphs for short circuit frequencies for standard GMAW (a) and CMT (b).

Table 6. Short Circuit Frequencies (SCFs) for the CMT process.

Sample	SCF (Hz)			
	1st Pass	2nd Pass	3rd Pass	Average \pm Std. Deviation
CMT	90.12	88.83	89.24	89.40 \pm 0.66

The temperature distributions for the first pass of the standard GMAW and for the CMT processes are presented in Figure 4. The analyses present the temperatures registered during the welding process and the cooling rate until the base material reached approximately 200 °C. Although the temperature gradient is very high at the weld area and some errors of the thermocouple location can have great influence on the peak temperature, the thermocouple located 2 mm from the root opening registered a peak of temperature around 1090 °C for the GMAW process, while the maximum temperature for the CMT process was around 930 °C. It can be seen that the cooling times t_{85} (time spent between 800 °C and 500 °C) were 15.3 s (19.6 °C/s on average) and 62 s (4.8 °C/s on average) for the GMAW and the CMT processes, respectively. These differences suggest that wire deposition was more pronounced in the CMT process.

Although the arc energy of both processes presented similar values (estimated heat input presented in Table 5), the standard GMAW process seemed to transfer more energy to the base material, with the thermocouple registering a higher peak in temperature. This could relate to the differences in voltage and current between the processes, although the welding speed was fixed for comparison. Microscopic investigations into the welding cross-section revealed the differences in material deposition for both processes (Figure 5).

The analysis based on the macrographs presented in Figure 5 confirms the slightly pronounced bead observed by visual inspection, with a height of about 3.33 mm for standard GMAW versus 4.09 mm for CMT (arrow B in Figure 5a,c). The wetting angle was also higher for the CMT process compared to standard GMAW, with about 95° compared to 65°, respectively. The welding width was also larger for the CMT process, with values of 14.95 mm versus 13.79 mm for GMAW. However, with these parameters, the joints prepared using the CMT process were not able to achieve full penetration, as observed in the GMAW process, despite the fact that no root reinforcement was observed. All these aspects and the estimated welding parameters presented in Table 5 confirm the characteristics of the CMT process to have a less-open arc during the process, which could be related to the high wetting angle and lower penetration depth when compared to the GMAW process. Thus, less heat was transferred to the base material, which indicates that the molten metal drop

solidified too fast when contact occurred. All measured instances of penetration and areas shown in Figure 5 are presented in Table 7.

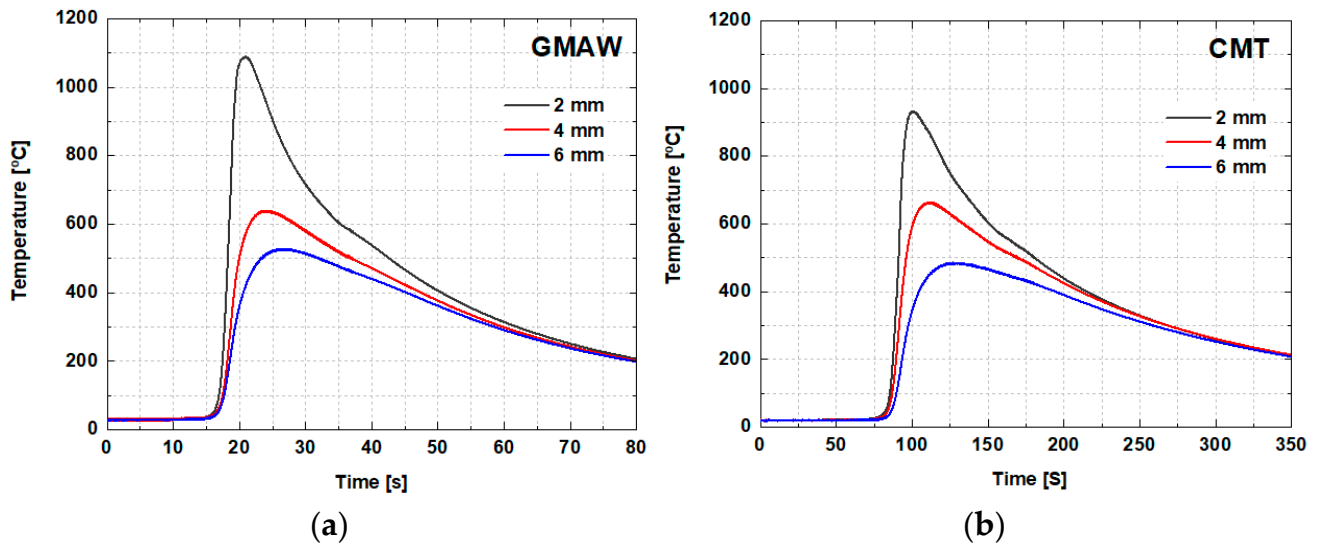


Figure 4. Temperature for the first pass of the (a) standard GMAW process and (b) the CMT process.

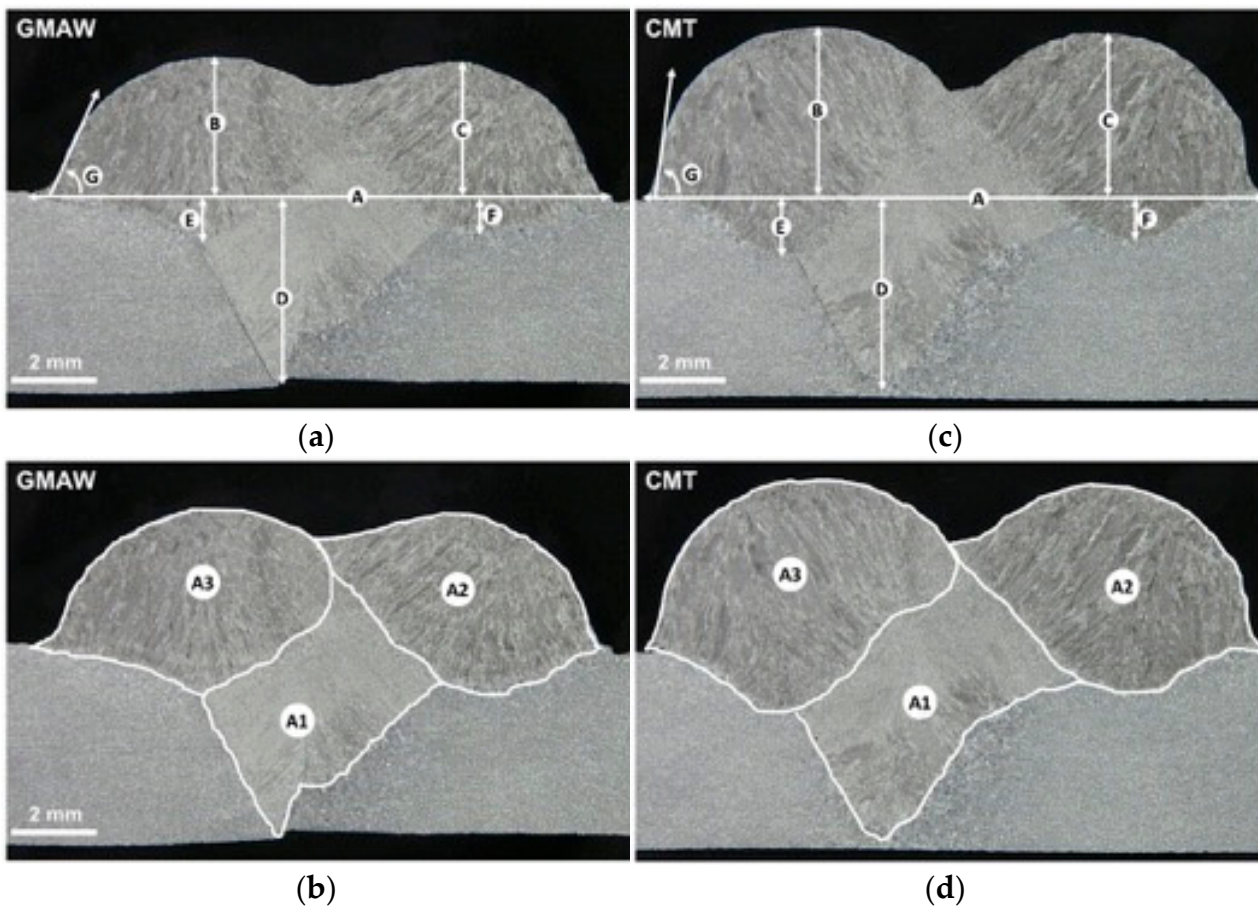


Figure 5. Optical macrographs showing the welding cross-section for standard GMAW (a,b); and for the CMT joints (c,d). The highlighted letters on each macrograph are the main area and dimensions related to each welding pass and are presented in Table 7.

Table 7. Area and dimensional measurements of the cross-section positions highlighted in Figure 5.

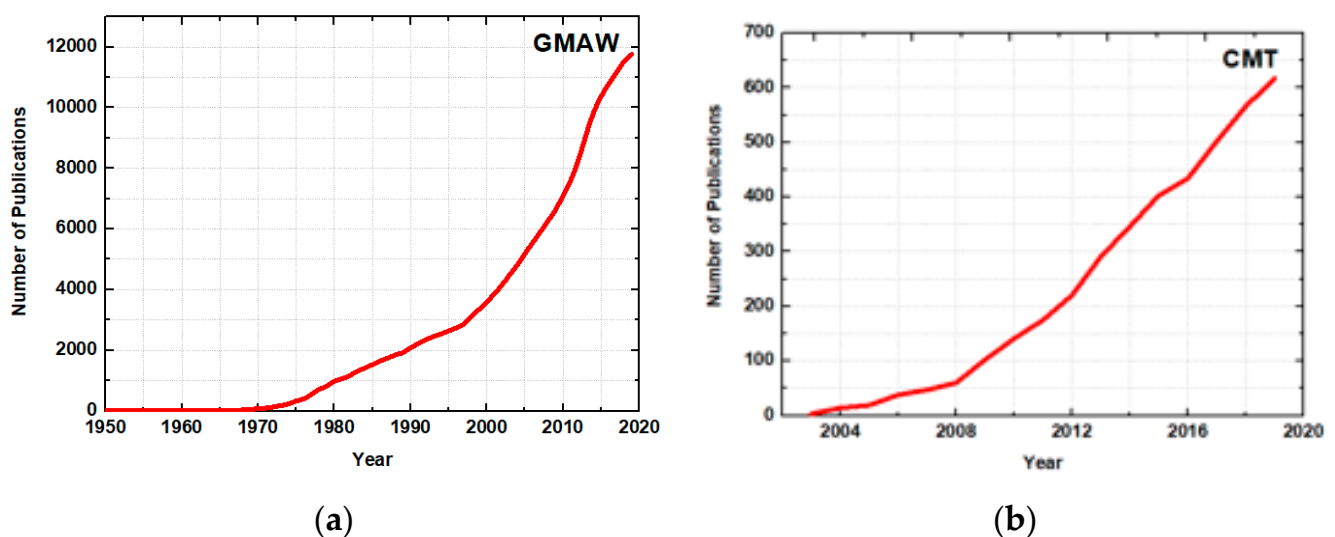
Sample	Positions Highlighted in Figure 5						
	A (mm)	B (mm)	C (mm)	D (mm)	E (mm)	F (mm)	G (°)
GMAW	13.79	3.33	3.18	3.29	4.55	1.05	65
CMT	14.95	4.09	3.98	4.30	1.42	1.05	95
	A1 (mm ²)	A2 (mm ²)	A3 (mm ²)	Total Average Area (mm ²)	Total Molten BM Area (mm ²)	Total Molten Joint Area (mm ²)	
GMAW	20.50	16.16	17.58	18.08	19.54	54.23	
CMT	25.95	20.14	23.26	23.11	21.57	69.35	

As also cited by Imoudu [48], these results confirm the characteristics of the CMT process, showing that by operating at the same level of heat input, the material deposition is higher than that of GMAW. Here, the choice of a higher wire feed results in a lower voltage and a higher current in the CMT process, even though the same welding speed was applied in both processes. In terms of welding characteristics, both processes showed similar depth penetration and morphologies for all passes. These results seem to be related to the high average current observed for the CMT process and the higher voltage of standard GMAW, which was expected based on the setup parameters and technological characteristics and was also suggested by other authors such as Haelsig et al. [31], Mezrag et al. [45], Pepe et al. [32], and Selvi et al. [6]. In terms of dilution, the calculation based on the estimated areas (the total molten base material area divided by the total molten joint area) shows that the GMAW values are of about 15% higher than the CMT process, which is in accordance with the literature, G.P. et al. [49].

4.2. TLC Analyses and Assessment of Technological Maturity

4.2.1. The Dataset Characteristics

The DII patent database used in this work revealed the existence of 11,352 related patents with standard GMAW and 535 with the CMT process [50]. The distribution of the requested patents over the years can be seen in Figure 6, and the observed disparity between the numbers for each process can be considered normal since the first technology (GMAW) was launched in the 1950s, while the second (CMT) was launched in the 2000s.

**Figure 6.** The number of accumulated patents related to the (a) standard GMAW and (b) CMT welding processes.

For the GMAW process (Figure 6a), the analysis revealed that the first patent was dated 1950, is owned by the Air Reduction Company, and was invented by Muller [51]. In terms of technological maturity, based on the phases presented in Figure 1, the curve in Figure 6a shows characteristics similar to those of the maturity or growth phases. On the other hand, CMT technology is considered relatively recent, as its patent registration is dated to 2003, and it was invented by Artelsmair [52]. By matching this result with the S-curve concept of the TLC presented in Figure 1, apparently, this technology is located within the growth phase of the curve (Figure 6b).

Considering the distribution of patents by country, Japan, China, and the United States hold the top three spots for both GMAW and CMT welding process requests (Table 8). From a business point of view, the company Fronius Int has about 162% more records on the CMT process than their closest competitor, Unitec Technologies Corp. [53]. Similar results were found for the GMAW process, with Illinois Tool W. Inc. showing 103% more patents than their closest competitor. Thus, in these particular cases, there is a high concentration of patents among these leading competitors.

Table 8. Countries and top assignees with a great number of patent depositions for CMT and GMAW welding technologies.

Country	GMAW	CMT	Top Assignees	GMAW	Top Assignees	CMT
Japan	2129	37	Illinois Tool W. Inc.	1821	Fronius Intern.	97
China	2035	252	Lincoln Elet. H. Inc.	897	United Tech. Corp	37
United States	1734	68	Kobe Steel Ltd.	327	Magna Intern. Inc.	29
Canada	608	9	L'air Liquide S.A.	294	GE Company	29
Germany	601	35	Victor Tech. H. Inc.	272	Siemens	22
Korea	462	15	Nippon Steel Corp.	206	Tianjin Univ.	20

A close look on the dataset presented in Figure 6 reveals that the most relevant and state-of-the-art technologies in this field cover different applications: (a) welding, soldering, and repairing; (b) tools, heat exchangers, assembly, robots, and gas turbines engines; and (c) gas turbines engines, airfoils, and turbomachines. These clusters of technologies and applications represent about 87% of the results for CMT technology. According to Ljung et al. [53], a larger percentage of technological interest indicates a saturation in that space, whereas lower rates indicate diverse technological representation. Thus, these results suggest a certain saturation and concentration of CMT technology.

4.2.2. Development of TLC Models and Analyses

Based on the methodology presented in Section 2 and Figure 6a,b, no seasonality factor can be observed for the two curves, which means that no external influences, such as weather, holidays, or periodic and repetitive facts, impact the “shapes” of the curves. Therefore, the use of the time-series method by applying triple exponential smoothing algorithms was not feasible for this dataset. This was confirmed when the tests for this model were conducted in the R Studio environment for both technologies: “Error in ets (dados, model = “AMN”): Forbidden model combination“. Thus, the use of the triple exponential smoothing method (time-series), highlighted in Table 4, will not be considered in this study.

CMT Technology

The performance of different algorithms using the time-series models presented in Table 4 is shown in Table 9. The main variables analysed were the root mean square error (RMSE), as suggested by Yilmaz [42]; the mean absolute error (MAE); and the mean absolute percentage error (MAPE), suggested by Myttenaere et al. [54]. The Akaike information criterion (AIC) was also used for the evaluations, and its values consider the number of parameters of the models, penalising the models with more parameters according to the

parsimony described in Bozdogan [44]. As the p -value for the Auto-ARIMA model was higher than 5% (Table 9), the null hypothesis of white noise was not rejected [27]. The results revealed that Auto-ARIMA is the best model for fitting the CMT patent dataset, since in all metrics (RMSE, MAE, MAPE, and AIC), auto-ARIMA showed the best results.

Table 9. CMT—Performance metrics for time-series models.

Time-Series Models	RMSE	MAE	MAPE	AIC	p -Value
Exponential—Simple	38.194	28.122	26.547	178.020	0.0008
Exponential—Double	10.042	7.184	20.302	136.590	0.6534
ARIMA	21.827	15.953	17.152	151.870	0.0656
Auto-ARIMA	10.038	7.118	13.776	115.640	0.6402

The next step was to use the Auto-ARIMA model to prepare the Ljung-Box Q statistical test proposed by Ljung and Box [55] and to test whether the series of observations (residuals from the fitted models) was random and independent over time. The R functions `qqnorm(.)` and `qqline(.)` were used to generate the curve (normal probability plot of residuals) presented in Figure 7, which showed normally distributed data along the fitting line, following the criteria of Kabacoff [27].

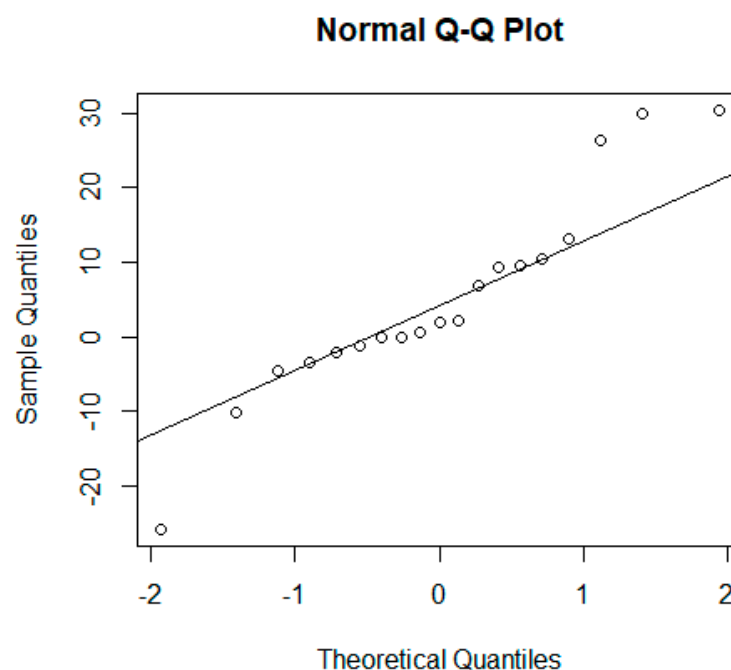


Figure 7. CMT normal probability plot of residuals for the Auto-ARIMA model.

For the growth-curves, the following models were tested according to Table 4: logistic, exponential, Richards, Baranyi, and Gompertz. All the results are presented in Figure 8, and the analyses indicate that the exponential (Figure 8c) and Gompertz (Figure 8f) models presented the worst fit, with many points outside the line.

Each model's performance is described in Table 10. The Richards model shows the best outcome for all indicators, with a lower AIC and RMSE and a larger R-squared— R^2 . As already mentioned, the AIC criterion is very relevant in this kind of comparison process because it considers the numbers of parameters in the models, penalising the models with more parameters according to the parsimony criteria described in Bozdogan [44].

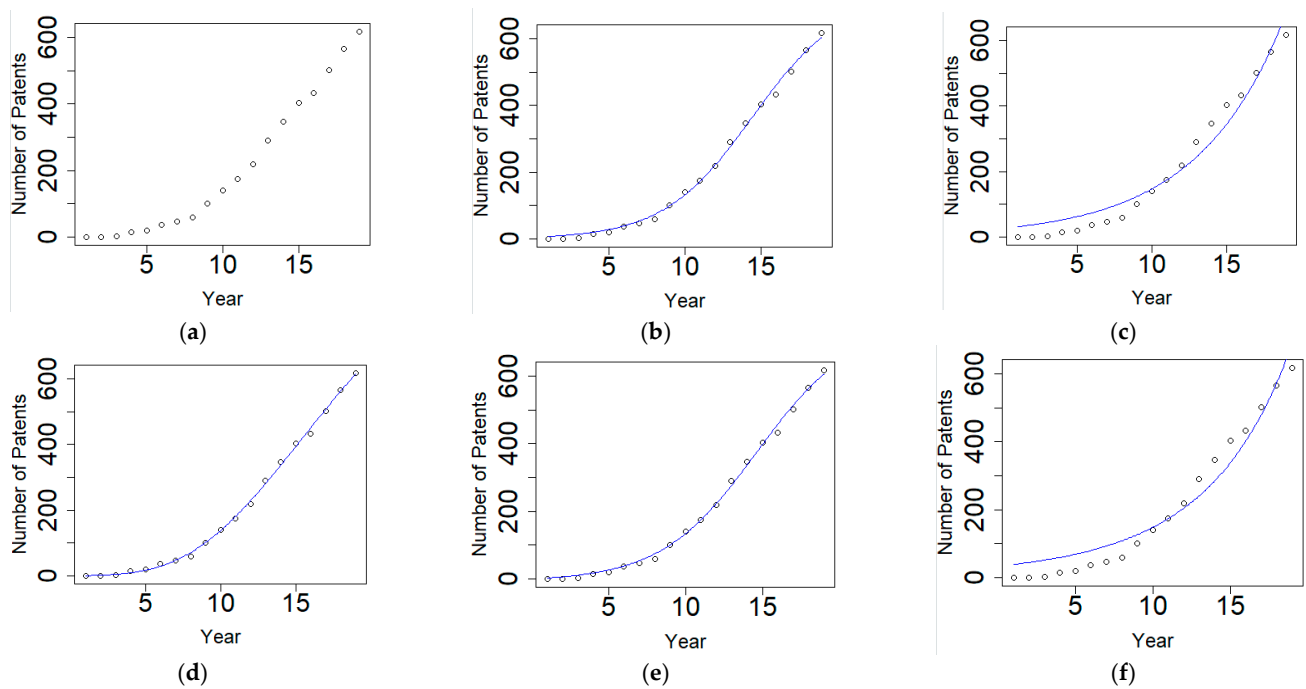


Figure 8. Patents CMT—Graphical analysis of growth models: (a) Original, (b) Logistic, (c) Exponential, (d) Richards, (e) Baranyi, and (f) Gompertz.

Table 10. CMT—Performance metrics for growth models.

Growth-Curve Models	RMSE	AIC	R ²	Parameters
Logistic	10.312	68.803	0.998	3
Exponential	37.603	88.155	0.968	2
Richards	7.045	64.511	0.999	4
Baranyi	9.152	68.834	0.998	4
Gompertz	42.487	92.170	0.960	3

Using the Best Models to Forecast

At this stage, a comparative test was made between the two best models for each type of technique: Auto-ARIMA for time-series and Richards for growth-curves. The last three years were removed from each dataset, and then we used the models to predict the years 2017, 2018, and 2019. The results are shown in Table 11. Here, the Richards growth model best fit the predictions for the following years since it had a lower value of RMSE.

Establishing the Curve and Its Inflection Points

After defining all the parameters for the Richards growth-curve function, as mentioned in item 2.2.3, the formula was completed as described in Equation (3):

$$P = 1885.67 \times \left(1 + 0.11926 \times e^{(-0.1123 \times t)}\right)^{-78.8003} \quad (3)$$

where P represents the number of accumulated patents in a specific year (t).

Table 11. CMT—Comparison between Growth-curve and Time-series models.

Year	Patents	Richards	AUTOARIMA
2107	502	489	465
2018	566	539	496
2019	617	587	527
	RMSE	24.75	69.21

To obtain the curve's inflection points, derivative mathematical concepts were applied. The application of mathematical methods was used to obtain the points of inflection of the curve, thereby determining the divisions between the stages of maturity of each technology. The second derivative is the fundamental concept of the central inflection point or change in the curve's concavity. Da Costa and Guerra [56] noted that when the second derivative of a given function is equal to zero, there is an inflection of its concavity at this point. Thus, the following rules were applied:

- Let f be a derivative function up to 2nd order in the interval I and suppose that at $x_0 \in I, f''(x_0) \neq 0$. In this case, if $f''(x_0) > 0$, then the curve of f has a positive concavity in x_0 ; otherwise, the curve of $f''(x_0) < 0$ has a negative concavity in x_0 ;
- Let f be a derivative function up to 2nd order in an interval I and suppose that $x_0 \in I$ is the abscissa of an inflection point in the curve of f . Thus, $f''(x_0) = 0$.

For the other inflection points, a third derivative concept was used. This concept is known as "Jerk" and is widely applied in physics. The time rate of the acceleration change is called the Jerk and is essential in mechanical and acoustic applications. The third derivative is the rate of change of the slope. When this rate is zero, the second derivative is constant, and the rate of the slope change is fixed, as defined by Schot [57]. In terms of the S-curve (Figure 6), this interpretation is related to the curve's acceleration changes. This means that between the emergent and growth phases, there is a spike in acceleration; from there, acceleration begins to decrease. In this transition, the first inflection or the first root of function d''' is equal to zero. In the transition between the maturity and saturation phases, a new inflection occurs. This new inflection is represented by the second root of the function when d''' is equal to zero. The inflection passes then through a negative peak of deceleration and gradually reduces, tending towards zero at its limit.

Figure 9 shows the real curve of CMT technology patents until 2019, plotted with the predicted curve using the formula obtained by the Richards growth-curve (Equation (3)). This curve best represented the data obtained from the patents. Adding the inflection points gives a clearer view of the behaviour of the technology and its possible predictions. As can be seen, this technology is already in a stage of maturity. Notably, based on this analysis, CMT technology could possibly reach saturation in the following years. This is a somewhat surprising finding for such a recent technology.

GMAW Technology

Table 12 shows the performance metrics calculated for each of the possibilities of the studied time-series models. Again, Auto-ARIMA appears to be the best model for fitting, except for the MAE indicator, which shows the Double Exponential method to be the best. However, the Double Exponential method has a Ljung-Box p -value < 0.05 , so, as proposed by Ljung and Box [55], it rejects the white noise hypothesis. This analysis methodology was followed by using Auto-ARIMA for the GMAW patent dataset.

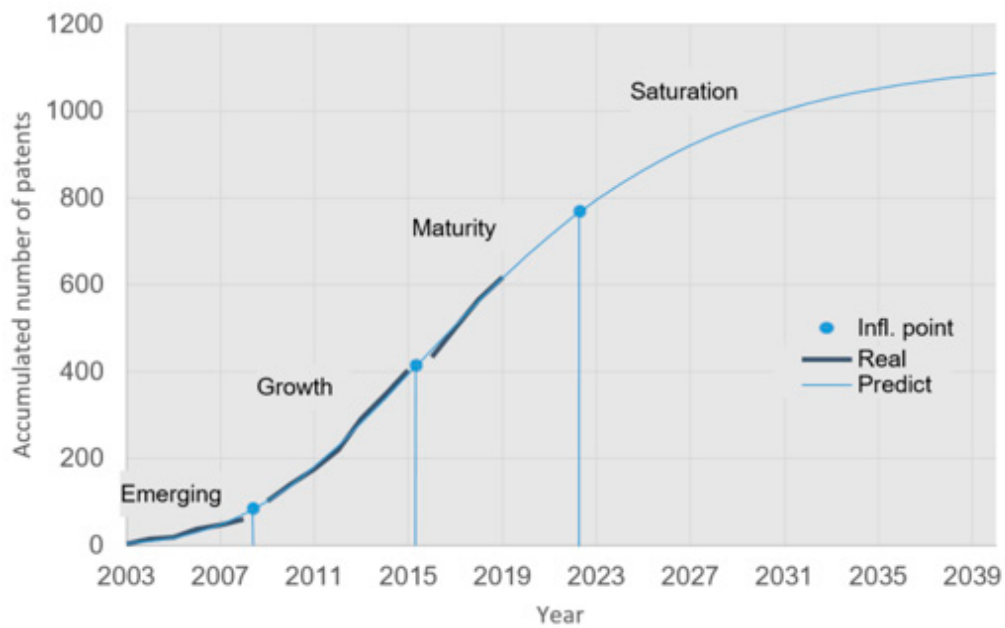


Figure 9. CMT—Actual patents (up to 2019), predicted curve, and inflection points.

Table 12. GMAW—Performance metrics for time-series models.

Time-Series Models	RMSE	MAE	MAPE	AIC	<i>p</i> -Value
Exponential—Simple	262.115	180.853	12.446	1001.670	4.109×10^{-15}
Exponential—Double	53.802	31.481	10.913	799.420	0.007567
ARIMA	140.798	93.383	7.074	822.000	4.501×10^{-9}
Auto-ARIMA	50.495	32.042	4.311	676.260	0.9291

In Table 12, the *p*-value for the Auto-ARIMA model was again higher than 5%, thus not rejecting the null hypothesis of the Ljung-Box test proposed by Ljung and Box [55]. The R functions qqnorm(.) and qqline(.) produced the graph (normal probability plot of residuals) in Figure 10. The results were satisfactory once the Auto-ARIMA case data were normally distributed along the fitting line following the criteria of Kabacoff [27].

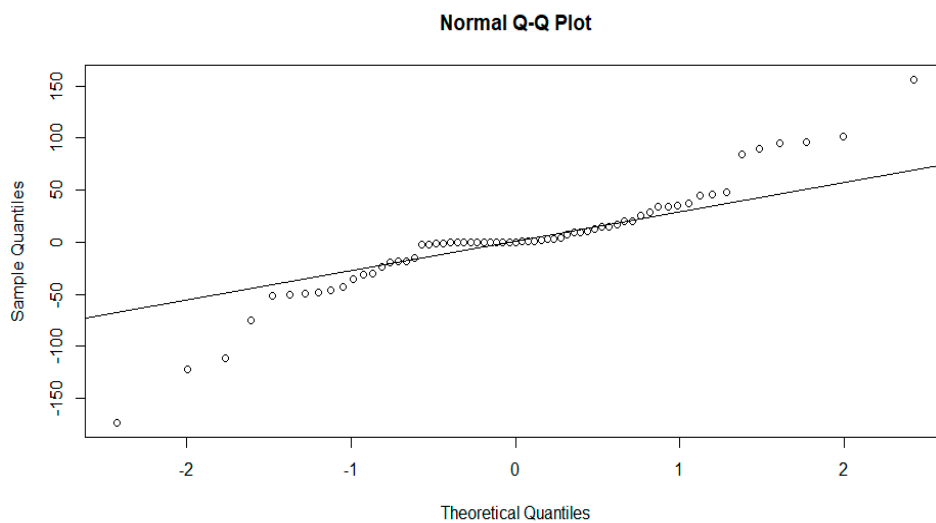


Figure 10. GMAW—Normal probability plot of residuals for Auto-ARIMA model.

For the growth-curve models, the same nonlinear methodology was applied to study the GMAW technology patents. Figure 11 shows that the Gompertz model offers the worst fit, as many points are outside the predicted line.

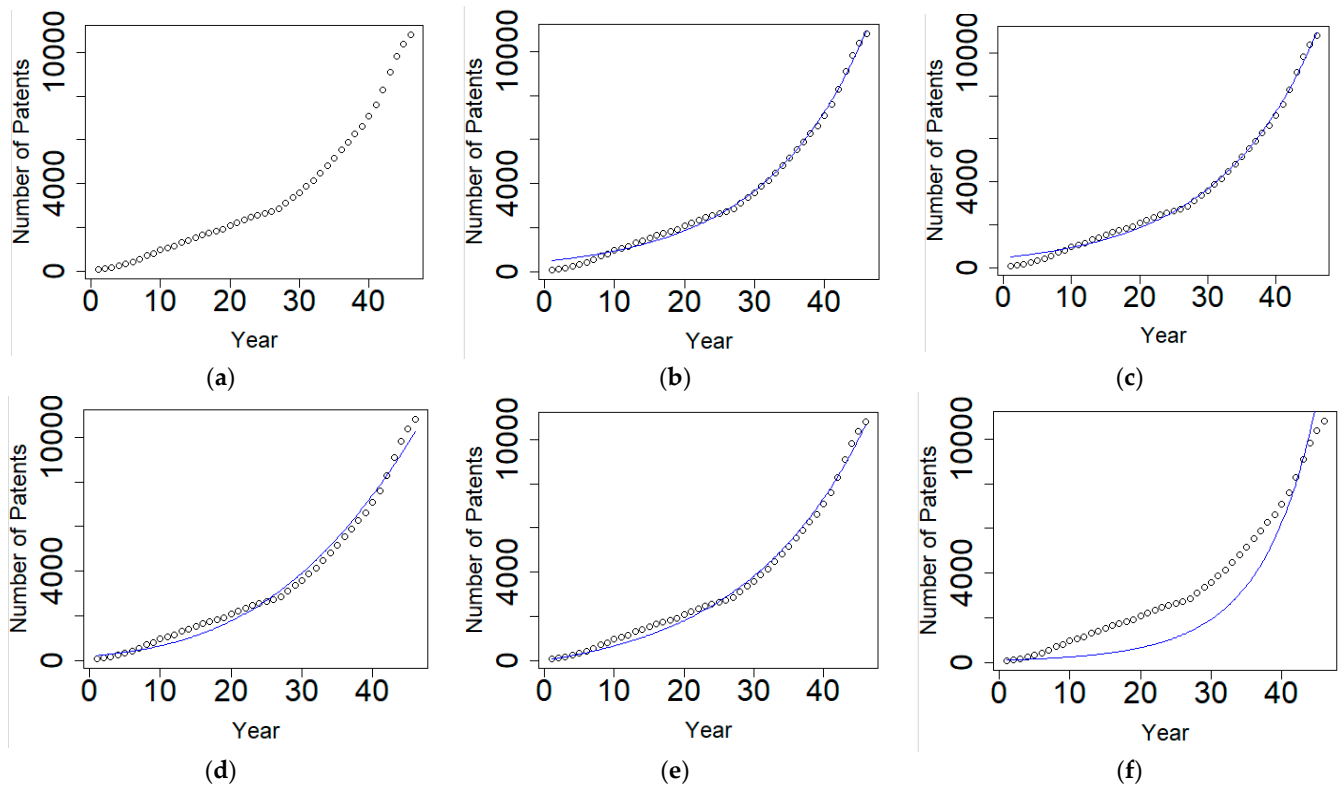


Figure 11. GMAW patents—Graphical analysis for the growth models. (a) Original; (b) Logistic; (c) Exponential; (d) Richards; (e) Baranyi; and (f) Gompertz.

Table 13 describes each growth curve model's performance results using the same algorithm in R studio. In this case, the Baranyi model presented better outcomes for all indicators: R^2 , RMSE, and AIC.

Table 13. GMAW—Performance metrics for the growth-curve models.

Growth-Curve Models	RMSE	AIC	R^2	Parameters
Logistic	0.995	243.183	392.020	3
Exponential	0.993	297.056	400.275	2
Richards	0.993	285.739	402.285	4
Baranyi	0.996	220.518	389.007	4
Gompertz	0.942	997.252	464.339	3

Using the Best Models to Forecast

At this stage, a test for comparison was made between both best-fitted models for each type of technique: Auto-ARIMA for time-series and Baranyi for growth-curves. The last three years were removed from the GMAW dataset to proceed with the predictions for 2017, 2018, and 2019. It can be seen, according to Table 14, that the Auto-ARIMA time-series model best fits the predictions for the following years, presenting a lower RMSE.

Table 14. GMAW—Comparison between the Growth and Time-series models.

Year	Patents	Baranyi	AUTOARIMA
2107	11,154	11,531	11,202
2018	11,513	12,302	11,613
2019	11,755	13,122	12,023
	RMSE	936.96	167.71

Establishing the Curve and Its Inflection Points

Following the methodology described in the previous section, we calculated and plotted the second and third derivatives in Figure 12. However, due to the Auto-ARIMA time-series models' characteristics, several roots emerged, as shown in Figure 12, leading to an unfeasible solution.

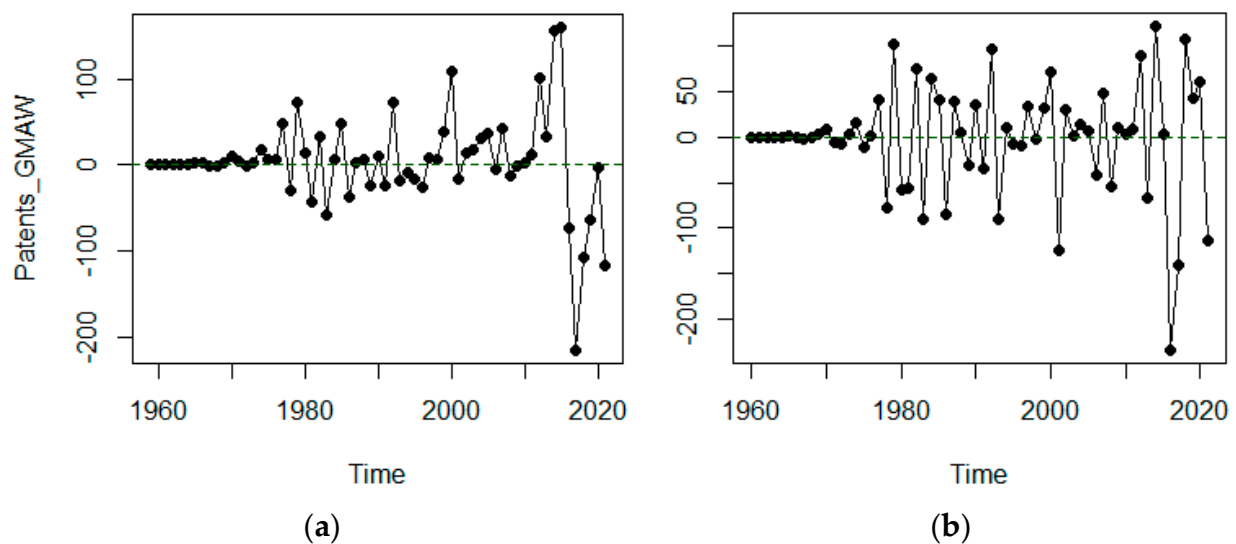


Figure 12. Plots of the 2nd (a) and 3rd (b) derivatives of the Auto-ARIMA function fit for the GMAW patents.

The analyses were conducted by plotting the graphical positioning using the second-best option: the Baranyi growth-curve. This decision was made once the Baranyi model presented consistent results, showing an even better (i.e., lower) AIC than the Auto-ARIMA model. Figure 13 illustrates the plot using the (estimated) parameters for the Baranyi model with its formula. The inflection points are the roots of the second and third derivatives, following the same methodology used for the CMT technology. Even though GMAW is an older technology, the results reveal that this technology is in the curve-growth phase. This suggests that GMAW is a key technology, showing that there is still room for further expansion compared to CMT technology, as noted in a similar analysis for another technology by Wilder et al. [12].

Notably, the CMT and GMAW welding technologies present inherent characteristics, as detailed in Table 15. As observed and stated by G.P. et al. [49], the CMT process offers the main advantage of low heat input and, therefore, lower dilution and spatter levels. On the other hand, this characteristic also limits the process in certain applications because of the chosen welding parameters, as reported by Imoudu [48]. Compared with the CMT process, the main advantage of the GMAW process is that it can be easily automated and integrated with other technologies. This is in full accordance with the TLC results, which indicates that GMAW has room for further expansion.

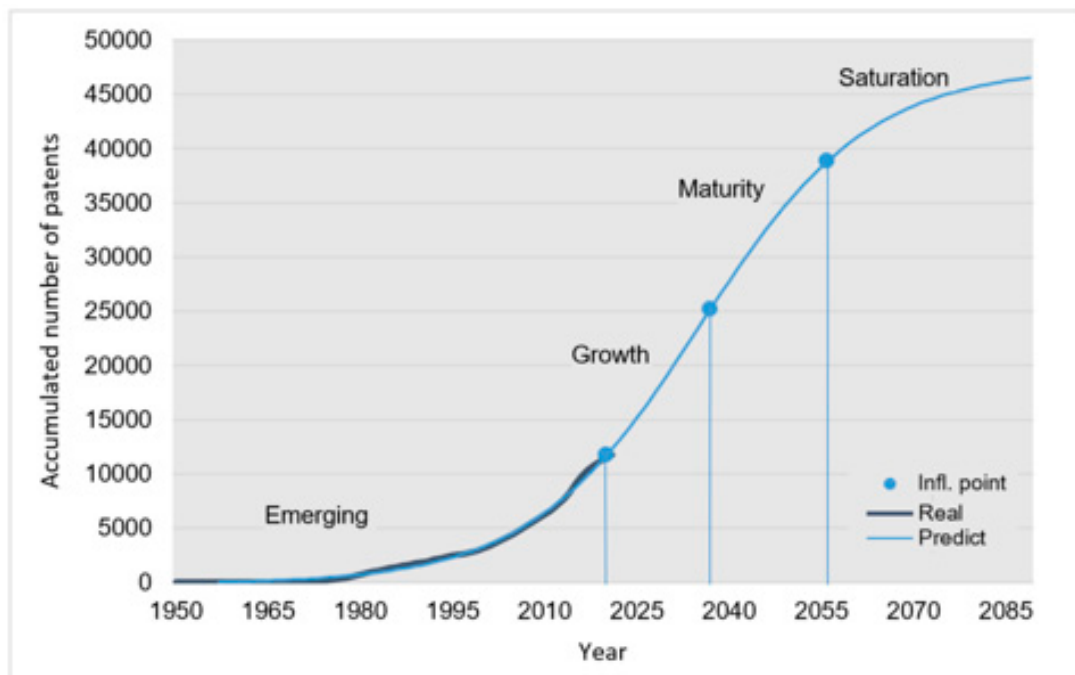


Figure 13. GMAW—Actual patents (up to 2019), predicted curve, and inflection points.

Table 15. Main applications, advantages, and limitations of the CMT and GMAW processes.

Welding Technology	Applications	Advantages	Limitations
Cold Metal Transfer (CMT)	<ul style="list-style-type: none"> Automotive industries; Defence sectors; Power plants as a method of additive manufacturing; Cladding, additive manufacturing, composite joint pin fabrication, and crack repair welding. 	<ul style="list-style-type: none"> Distortion reduction; Increased productivity; Low heat input; Low levels of dilution; Spatter free welding; Perfect arc length management compared with the traditional process which measured by weld voltage. 	<ul style="list-style-type: none"> Low precision in shaping; Short circuit phenomena do not exist for greater currents; The upper limits of the application are close to those of the conventional short arc process, i.e., when the transition zone starts.
Gas Metal Arc Welding (GMAW)	<ul style="list-style-type: none"> Widely used in the manufacturing industry; Industrial manufacturing; Agriculture; Construction industry; Shipbuilding; Marine and ground vehicle industries; Mining. 	<ul style="list-style-type: none"> Low cost; Easy operation; Good adaptability; High productivity; Narrow heat-affected zone; Concentration of heat source; Low deformation; High welding efficiency; Good protection; No need to use a welding flux; Easily automated. 	<ul style="list-style-type: none"> After welding, due to the effect of high temperatures, defects usually appear in the welded parts; Reduced control level; The arc must be protected against draught; Spatter formation.

5. Conclusions

In this study, GMAW and CMT welding processes were investigated in terms of their basic welding characteristics and maturity levels based on patent records using TLC analysis. Based on the results, the following conclusions can be drawn:

5.1. Welding Characteristics

- Visual inspection revealed a good welding bead with a lack of superficial defects and discontinuities for both processes. The chosen parameters ensured similar heat inputs in both prepared joints, and the analyses showed that the CMT process promoted a high deposition rate and less heat transfer to the base material compared to standard GMAW. This supported the lack of penetration and the pronounced welding bead observed for the CMT joints;
- The short circuit frequency analyses confirmed the stable and controlled material deposition under the CMT process, revealing a distinct frequency for material transfer. The monitored voltage and current parameters revealed the three typical phases connected with peaks of current and arc reignition after the filler material melted. At that moment, a small droplet of molten metal was detached, followed by a voltage reduction;
- The monitored temperature profile confirms that the GMAW process promoted high temperature peaks and cooling rates, which led to a high heat transfer to the base material with peaks of current when the arc reignited after the short circuit phase.

5.2. TLC Analyses

- The patent dataset developed and used in this study revealed that GMAW technology has more than twenty times the number of patents of CMT. This may be connected with the high possibility of adjustment, automation, and time use with this technology. The main clusters of the request themes/topics were related to the methodology, characteristics, and applications. The analyses also revealed that few countries and companies dominate patent deposition in the field of CMT welding technology. This scenario offers a great opportunity for other countries and companies to study and deliver new solutions to the market in this regard.
- The use of advanced models to predict the S-curve trends revealed that, for the CMT process, the formula obtained by Richards growth-curve was the one that best represented the data obtained from the patents. Instead, for the GMAW process, the growth-curve model using the Baranyi methodology was the one that best fit with the original data. Both models differed mainly in their algorithms for inflection points, thus providing a clearer view of the behaviour of the technology and its possible predictions;
- The S-curve trend for the CMT process revealed that, despite being recent, the technology is already in a mature phase, a fact confirmed by the experts' opinions due to the limited use of this technology. For the GMAW process, despite being older, this technology is positioned in the growth phase on the S-curve, indicating great possibility for advancement—a fact also supported by the opinions of the experts.
- The results confirm that mathematical modelling can precisely reveal the inflection points and phases of each technology, which provides a new possible perspective of analysis in terms of maturity level. This kind of methodology together with the experts' opinion can be essential for assisting in the decision-making and analysis of technological trends.

The findings presented in this study have demonstrated the importance of engaging in a broader analysis when comparing different process technologies. This evaluation, from a technical perspective, has fundamental importance in establishing the relevant limits, but technological maturity level analyses can present a broader overview of perspectives to obtain forecasting and help in the decision-making market process. It must be highlighted that, to increase the reliability of the models, other variables should be added to provide a more robust analysis in terms of TLC.

Author Contributions: Conceptualization, A.S.O., R.O.d.S. and R.S.C.; methodology, A.S.O., R.O.d.S., E.L.D., P.H.F.d.S. and R.S.C.; validation, E.L.D., P.H.F.d.S. and R.S.C.; formal analysis, A.S.O. and R.O.d.S.; investigation, A.S.O. and R.O.d.S.; resources, A.S.O., B.C.d.S.S. and R.S.C.; data curation, A.S.O. and R.O.d.S.; writing—original draft preparation, A.S.O. and R.O.d.S.; writing—review and editing, B.C.d.S.S., L.L.N.G., M.A., U.R., R.R.S., B.A.S.M., E.L.D., P.H.F.d.S. and R.S.C.; visualization, A.S.O., R.O.d.S., B.A.S.M. and R.S.C.; supervision, U.R., R.R.S., E.L.D., P.H.F.d.S. and R.S.C.; project administration, A.S.O., B.C.d.S.S., R.R.S. and R.S.C. All authors have read and agreed to the published version of the manuscript.

Funding: This research received no external funding.

Conflicts of Interest: The authors declare no conflict of interest.

References

1. Yapp, D.; Blackman, S.A. Recent Developments in High Productivity Pipeline Welding. *J. Braz. Soc. Mech. Sci. Eng.* **2004**, *26*, 89–97. [[CrossRef](#)]
2. Shen, H.; Deng, R.; Liu, B.; Tang, S.; Li, S. Study of the mechanism of a stable deposited height during GMAW-based additive manufacturing. *Appl. Sci.* **2020**, *10*, 4322. [[CrossRef](#)]
3. Goede, M.; Stehlin, M.; Rafflenbeul, L.; Kopp, G.; Beeh, E. Super Light Car—Lightweight construction thanks to a multi-material design and function integration. *Eur. Transp. Res. Rev.* **2009**, *1*, 5–10. [[CrossRef](#)]
4. Madhavan, S.; Kamaraj, M.; Vijayaraghavan, L. Microstructure and mechanical properties of cold metal transfer welded aluminium/dual phase steel. *Sci. Technol. Weld. Join.* **2016**, *21*, 194–200. [[CrossRef](#)]
5. Cornacchia, G.; Cecchel, S.; Panvini, A. A comparative study of mechanical properties of metal inert gas (MIG)-cold metal transfer (CMT) and fiber laser-MIG hybrid welds for 6005A T6 extruded sheet. *Int. J. Adv. Manuf. Technol.* **2018**, *94*, 2017–2030. [[CrossRef](#)]
6. Selvi, S.; Vishvakshenan, A.; Rajasekar, E. Cold metal transfer (CMT) technology—An overview. *Def. Technol.* **2018**, *14*, 28–44. [[CrossRef](#)]
7. Zhang, H.T.; Feng, J.C.; He, P.; Zhang, B.B.; Chen, J.M.; Wang, L. The arc characteristics and metal transfer behaviour of cold metal transfer and its use in joining aluminium to zinc-coated steel. *Mater. Sci. Eng. A* **2009**, *499*, 111–113. [[CrossRef](#)]
8. Pickin, C.G.; Williams, S.W.; Lunt, M. Characterisation of the cold metal transfer (CMT) process and its application for low dilution cladding. *J. Mater. Process. Technol.* **2011**, *211*, 496–502. [[CrossRef](#)]
9. Costa, T.F.; Benedetti Filho, E.; Arevalo, H.D.H.; Vilarinho, L.O. Assessment of Conventional and Controlled Short-Circuit MIG/MAG Processes for Steel-Pipe Welding in Single Pass. *Soldag. Inspeção* **2012**, *17*, 356–368. [[CrossRef](#)]
10. Chang, Y.J.; Sproesser, G.; Neugebauer, S.; Wolf, K.; Scheumann, R.; Pittner, A.; Rethmeier, M.; Finkbeiner, M. Environmental and Social Life Cycle Assessment of Welding Technologies. *Procedia Cirp* **2015**, *26*, 293–298. [[CrossRef](#)]
11. Taylor, M.; Taylor, A. The technology life cycle: Conceptualization and managerial implications. *Int. J. Prod. Econ.* **2012**, *140*, 541–553. [[CrossRef](#)]
12. Wilder, J.; Sossa, Z.; Palop, F.; Alzate, B.A.; Mauricio, F.; Salazar, V.; Felipe, A.; Patiño, A. S-Curve Analysis and the Technology Life Cycle: Application in Series of Data of Articles and Patents. *Espacios* **2016**, *37*, 19.
13. Little, A.D. The strategic management of technology. *Eur. Manag. Forums* **1981**, *1*, 1–39.
14. Wu, J.; Yang, Z.; Hu, X.; Wang, H.; Huang, J. Exploring driving forces of sustainable development of China's new energy vehicle industry: An analysis from the perspective of an innovation ecosystem. *Sustainability* **2018**, *10*, 4827. [[CrossRef](#)]
15. Gao, L.; Porter, A.L.; Wang, J.; Fang, S.; Zhang, X.; Ma, T.; Wang, W.; Huang, L. Technology life cycle analysis method based on patent documents. *Technol. Forecast. Soc. Chang.* **2013**, *80*, 398–407. [[CrossRef](#)]
16. Xin'an, W.; Aijun, M. Comparison of four nonlinear growth models for effective exploration of growth characteristics of turbot *Scophthalmus maximus* fish strain. *Afr. J. Biotechnol.* **2016**, *15*, 2251–2258. [[CrossRef](#)]
17. Madvar, M.D.; Khosropour, H.; Khosravianian, A.; Mirafshar, M.; Azaribeni, A.; Rezapour, M.; Nouri, B. Patent-based technology life cycle analysis: The case of the petroleum industry. *Foresight STI Gov.* **2016**, *10*, 72–79. [[CrossRef](#)]
18. Jamali, M.Y.; Aslani, A.; Moghadam, B.F.; Naaranoja, M.; Madvar, M.D. Analysis of photovoltaic technology development based on technology life cycle approach. *J. Renew. Sustain. Energy* **2016**, *8*. [[CrossRef](#)]
19. Fye, S.R.; Charbonneau, S.M.; Hay, J.W.; Mullins, C.A. An examination of factors affecting accuracy in technology forecasts. *Technol. Forecast. Soc. Chang.* **2013**, *80*, 1222–1231. [[CrossRef](#)]
20. Smith, M.; Agrawal, R. A Comparison of Time Series Model Forecasting Methods on Patent Groups. In Proceedings of the CEUR Workshop Proceedings, Rome, Italy, 24–25 November 2014; pp. 167–173.
21. Andrade, H.; Junior Chagas, M.; Silva, M.; Brito, M.A.; Rocha, D.; Ribeiro, J. *Avaliação da Maturidade Tecnológica: Conceitos*; Fbra, E.B.E., Ed.; Edição: Jundiaí, Brazil, 2019; ISBN 9786551040009.
22. Yang, X.; Yu, X.; Liu, X. Obtaining a sustainable competitive advantage from patent information: A patent analysis of the graphene industry. *Sustainability* **2018**, *10*, 4800. [[CrossRef](#)]
23. Kucharavy, D.; De Guio, R. Logistic substitution model and technological forecasting. *Procedia Eng.* **2011**, *9*, 402–416. [[CrossRef](#)]
24. De Gooijer, J.G.; Hyndman, R.J. 25 Years of Time Series Forecasting. *Int. J. Forecast.* **2006**, *22*, 443–473. [[CrossRef](#)]

25. Krispin, R. *Hands-On Time Series Analysis with R: Perform Time Series Analysis and Forecasting Using R*, 1st ed.; Shetty, S., Ed.; Packt Publishing: Birmingham, UK, 2019; ISBN 9781788629157.
26. Bouzada, M.A.C. Aprendendo Decomposição Clássica: Tutorial para um Método de Análise de Séries Temporais. *TAC Technol. Adm. Contab.* **2012**, *2*, 1–18. [[CrossRef](#)]
27. Kabacoff, R.I. *R in Action Data Analysis and Graphics with R*; Manning Publications: New York, NY, USA, 2011; ISBN 9781935182399.
28. Lobacz, A.; Kowalik, J.; Tarczynska, A. Modeling the growth of *Listeria monocytogenes* in mold-ripened cheeses. *J. Dairy Sci.* **2013**, *96*, 3449–3460. [[CrossRef](#)] [[PubMed](#)]
29. Lezama-Nicolás, R.; Rodríguez-Salvador, M.; Río-Belver, R.; Bildosola, I. A bibliometric method for assessing technological maturity: The case of additive manufacturing. *Scientometrics* **2018**, *117*, 1425–1452. [[CrossRef](#)] [[PubMed](#)]
30. EN, D. *Hot Rolled Products of Structural Steels Part 2: Technical Delivery Conditions for Non-Alloy Structural Steels*; DIN EN 10025-2; BSI: London, UK, 2005.
31. Haelsig, A.; Mayr, P.; Kusch, M. Determination of energy flows for welding processes. *Weld. World* **2016**, *60*, 259–266. [[CrossRef](#)]
32. Pepe, N.; Egerland, S.; Colegrove, P.A.; Yapp, D.; Leonhartsberger, A.; Scotti, A. Measuring the process efficiency of controlled gas metal arc welding processes. *Sci. Technol. Weld. Join.* **2011**, *16*, 412–417. [[CrossRef](#)]
33. Imoudu, N.E.; Ayele, Y.Z.; Barabadi, A. The characteristic of cold metal transfer (CMT) and its application for cladding. In Proceedings of the IEEE International Conference on Industrial Engineering and Engineering Management, the Arctic University of Norway, Bangkok, Thailand, 16–19 December 2018; Volume 2017-Decem, pp. 1883–1887.
34. Tomków, J.; Czupryński, A.; Czupryński, C.; Fydrych, D. The Abrasive Wear Resistance of Coatings Manufactured on High-Strength Low-Alloy (HSLA) Offshore Steel in Wet Welding Conditions. *Coatings* **2020**, *10*, 219. [[CrossRef](#)]
35. WIPO. *WIPO Guide to Using PATENT*; WIPO Publishing: New York, NY, USA, 2015; pp. 1–43.
36. RStudio Team. *RStudio: Integrated Development Environment for R*. Available online: <https://rstudio.com/products/rstudio/> (accessed on 10 March 2019).
37. Hyndman, R.; Athanasopoulos, G.; Bergmeir, C.; Caceres, G.; Chhay, L.; O'Hara-Wild, M.; Petropoulos, F.; Razbash, S.; Wang, E.; Yasmeen, F. *Forecast: Forecasting Functions for Time Series and Linear Models*. Available online: <http://pkg.robjhyndman.com/forecast%3E> (accessed on 10 March 2020).
38. Petzoldt, T. *Growthrates: Estimate Growth Rates from Experimental Data*; R Package: Auckland City, New Zealand, 2019; p. 42.
39. Anderson, E.C.; Winter, D.J. *Forecasting Functions for Time Series and Linear Models*. 2020, p. 140. Available online: <https://rstudio.com/products/rstudio/> (accessed on 10 March 2020).
40. Kucharavy, D.; De Guio, R. Application of logistic growth curve. *Procedia Eng.* **2015**, *131*, 280–290. [[CrossRef](#)]
41. Conservation, P. *Growth II—A Major Upgrade to Our “Simply Growth” Software. Fits and Plots von Bertalanffy, Gompertz, Logistic and a Wide Range of Other Growth Curves to Length and/or Weight at Age Data*; Pisces Conservation Ltd.: Hampshire, UK, 2006.
42. Yilmaz, M.T. Identifiability of Baranyi model and comparison with empirical models in predicting effect of essential oils on growth of *Salmonella typhimurium* in rainbow trout stored under aerobic, modified atmosphere and vacuum packed conditions. *Afr. J. Biotechnol.* **2011**, *10*, 7468–7479. [[CrossRef](#)]
43. Phillips, F. On S-curves and tipping points. *Technol. Forecast. Soc. Chang.* **2007**, *74*, 715–730. [[CrossRef](#)]
44. Bozdogan, H. Model selection and Akaike's Information Criterion (AIC): The general theory and its analytical extensions. *Psychometrika* **1987**, *52*, 345–370. [[CrossRef](#)]
45. Mezrag, B.; Deschaux-Beaume, F.; Benachour, M. Control of mass and heat transfer for steel/ aluminium joining using cold metal transfer process. *Sci. Technol. Weld. Join.* **2015**, *20*, 189–198. [[CrossRef](#)]
46. Zhang, H.; Hu, S.; Wang, Z.; Liang, Y. The effect of welding speed on microstructures of cold metal transfer deposited AZ31 magnesium alloy clad. *Mater. Des.* **2015**, *86*, 894–901. [[CrossRef](#)]
47. Dutra, J.C.; Gonçalves e Silva, R.H.; Marques, C. Melting and welding power characteristics of MIG–CMT versus conventional MIG for aluminium 5183. *Weld. Int.* **2015**, *29*, 181–186. [[CrossRef](#)]
48. Imoudu, N.E. *The Characteristic of Cold Metal Transfer (CMT) and Its Application for Cladding*; The Arctic University of Norway: Tromsø, Norway, 2017.
49. Rajeev, G.P.; Kamaraj, M.; Bakshi, S.R. Hardfacing of AISI H13 tool steel with Stellite 21 alloy using cold metal transfer welding process. *Surf. Coat. Technol.* **2017**, *326*, 63–71. [[CrossRef](#)]
50. Derwent Innovation Index—DII Derwent Innovation Index. Available online: <https://www.derwentinnovation.com/login/> (accessed on 16 August 2020).
51. Muller, A. *United States Patent Office Method of Arc Welding*; United States Patent and Trademark Office: Alexandria, VA, USA, 1950; p. 867.
52. Artelsmair, J. Unit Combining Welding Processes, Includes Separate, Synchronized Burners for Welding and Cold-Metal-Transfer Processes. U.S. Patent 20070145028A1, 15 December 2003.
53. WIPO; INSEAD; Cornell. *Global Innovation Index 2019*; WIPO: Geneva, Switzerland, 2019.
54. de Myttenaere, A.; Golden, B.; Le Grand, B.; Rossi, F. Mean Absolute Percentage Error for regression models. *Neurocomputing* **2016**, *192*, 38–48. [[CrossRef](#)]
55. Ljung, G.M.; Box, G. On a measure of lack of fit in time series models. *Biometrika* **1978**, *65*, 297–303. [[CrossRef](#)]
56. Da Costa, G.A.T.F.; Guerra, F. *Cálculo I*; 2ª Edição; UFSC: Florianópolis, Brazil, 2009; ISBN 978-85-99379-78-3.
57. Schot, S.H. Jerk: The time rate of change of acceleration. *Am. J. Phys.* **1978**, *46*, 1090–1094. [[CrossRef](#)]